Aerobic Capacity Mediates Susceptibility For The Transition From Steatosis To Steatohepatitis

E. Matthew Morris[1], Colin S. McCoin[1], Julie A. Allen[1], Michelle L. Gastecki[2], Lauren G. Koch[3], Steven L. Britton[3], Justin A. Fletcher[4], Xiarong Fu[4], Wen-Xing Ding[5] Shawn C. Burgess[4], R. Scott Rector[2,6], John P. Thyfault[1,7]

1 Department of Molecular & Integrative Physiology, University of Kansas Medical Center, Kansas City, Kansas, USA
2 Department of Nutrition and Exercise Physiology, University of Missouri, Columbia, Missouri, USA
3 Department of Anesthesiology, University of Michigan, Ann Arbor, Michigan, USA
4 Advanced Imaging Research Service[7], University of Texas Southwestern, Dallas, Texas, USA
5 Department of Pharmacology, Toxicology, and Therapeutics, University of Kansas Medical Center, Kansas City, Kansas, USA
6 Harry S. Truman Memorial Veterans Hospital-Research Service, Columbia, Missouri, USA
7 Kansas City VA Medical Center-Research Service, Kansas City, Missouri, USA

Keywords
steatohepatitis, aerobic capacity, inflammation, mitochondria, fatty acid oxidation

Running Title: Aerobic capacity impacts diet-induced steatohepatitis

Corresponding Author Information

John P. Thyfault, Ph.D.
Associate Professor
Department of Molecular and Integrative Physiology
3901 Rainbow Boulevard
Hemenway Life Sciences Innovation Center
Mailstop 3043
University of Kansas Medical Center
Kansas City, KS 66160
Phone:
Fax:
jthyfault@kumed.edu

Word Count: 4936

Number of Figure and Tables: 10

Disclosures – The authors have no conflicts of interest to disclose for this research.

Author Contributions: Author contributions: EMM, RSR, JPT, conception and design of research; JPT, approved research design; EMM, CSC, JAA, MLG, JAF, XF, performed experiments; EMM, CSC, JAA, MLG, JAF, XF, analyzed data; EMM, CSC, JAA, MLG, LGK, SLB, JAF, XF, WXD, SCB, RSR, JPT, interpreted results of experiments; EMM prepared manuscript; EMM, CSC, JAA, MLG, LGK, SLB, JAF, XF, WXD, SCB, RSR, JPT edited and revised manuscript.

Key Points Summary

- Low intrinsic aerobic capacity is associated with increased all-cause and liver-related mortality in humans.
- Low intrinsic aerobic capacity in the low capacity runner rat (LCR) increases susceptibility to acute and chronic high-fat/high-sucrose diet-induced steatosis, without observed increases in liver inflammation.
- Addition of excess cholesterol to a high-fat/high-sucrose diet produced greater steatosis in both strains. However, the LCR rat demonstrated greater susceptibility to increased liver inflammatory and apoptotic markers compared to high capacity runner rats (HCR).
- The progressive non-alcoholic fatty liver disease observed in the LCR rats following western diet feeding was associated with further declines in liver fatty acid oxidation and mitochondrial respiratory capacity compared to HCR.

Abstract

Background & aims: Low aerobic capacity increases risk for NAFLD and liver-related disease mortality, but mechanisms mediating these effects remain unknown. We recently reported that rats bred for low aerobic capacity (low capacity runner (LCR)) displayed susceptibility to high-fat diet-induced steatosis in association with reduced hepatic mitochondrial fatty acid oxidation (FAO) and respiratory capacity compared to high aerobic capacity (high capacity runners (HCR)) rats. Here we tested the impact of aerobic capacity on susceptibility for progressive liver disease following a 16 week 'western diet' high in fat (45% kcal), cholesterol (1% w/w), and sucrose (15% kcal). **Results:** Unlike previously with a diet high in fat and sucrose alone, the inclusion of cholesterol in the WD induced hepatomegaly, and steatosis in both HCR and LCR, while producing greater cholesterol ester accumulation in LCR compared to HCR. Importantly, WD-fed low-fit LCR rats displayed greater inflammatory cell infiltration, serum ALT, expression of hepatic inflammatory markers (F4/80, MCP-1, TLR4, TLR2, and IL-1b), and effector caspase (caspase-3 & -7) activation compared to HCR. Further, LCR rats had greater WD-induced decreases in complete FAO and mitochondrial respiratory capacity. **Conclusions:** Intrinsic aerobic capacity had no impact on WD-induced hepatic steatosis; however, rats bred for low aerobic capacity developed greater hepatic inflammation which was associated with reduced hepatic-mitochondrial FAO and -respiratory capacity and increased accumulation of cholesterol esters. These results confirm epidemiological reports that aerobic capacity impacts

progression of liver disease and suggest that these effects are mediated through alterations in hepatic mitochondrial function.

Introduction

Aerobic capacity, also termed cardiorespiratory fitness, is the most powerful predictor of cardiovascular and all-cause mortality independent of other major risk factors (Myers *et al.*, 2002). Low aerobic capacity is also an independent predictor for multiple metabolic disease states including non-alcoholic fatty liver disease (NAFLD) (Church *et al.*, 2006). Aerobic capacity is substantially reduced in NAFLD patients (Croci *et al.*, 2012), and low initial aerobic capacity negatively impacts lifestyle-induced treatment of NAFLD (Kantartzis *et al.*, 2009), increases mortality in chronic liver disease patients, and reduces survivability following liver transplant (Bernal *et al.*, 2014). However, potential mechanisms by which aerobic capacity mediates susceptibility to NAFLD and liver disease are not well understood.

High calorie, high fat diets (HFD) are associated with NAFLD risk and obesity in humans and are commonly utilized to induce hepatic steatosis in rodent models. However, chronic HFD-induced hepatic steatosis does not progress to NASH in rodent models (Matteoni *et al.*, 1999). Whereas, we and others have shown the addition of refined sugar and/or cholesterol to a HFD has been shown to induce non-alcoholic steatohepatitis (NASH)-like outcomes (Gan *et al.*, 2014; Bashiri *et al.*, 2016; Linden *et al.*, 2016). Inappropriate cholesterol metabolism has received considerable attention in human and animal studies of NAFLD, and has been observed to modulate multiple pathways triggering NASH development (Min *et al.*, 2012; Arguello *et al.*, 2015). In support of these findings, large epidemiological reports link elevated cholesterol consumption with increased risk of NASH (Musso *et al.*, 2003). Therefore, both intrinsic aerobic capacity and western diet (WD - high in fat, sugar, and cholesterol) clearly impact prevalence and progression of NAFLD severity including the transition to NASH, but the interaction of these factors has never been examined.

In order to assess the role of intrinsic aerobic capacity in modulating the susceptibility to WD-induced NASH, we utilized the high capacity runner (HCR)/low capacity runner (LCR) rat model system created by selective breeding for divergent intrinsic aerobic capacities (Koch & Britton, 2001; Ren *et al.*, 2013). We have previously shown that low intrinsic

aerobic capacity increases susceptibility for hepatic steatosis under chow and acute and chronic HFD conditions (increased lipids and sucrose), effects we have attributed to robust reductions in hepatic mitochondrial-content, -fatty acid oxidation (FAO) and -respiratory capacity (MRC) in LCR vs HCR rats (Thyfault *et al.*, 2009; Morris *et al.*, 2014; Morris *et al.*, 2016). The robust differences in hepatic mitochondrial oxidative capacity play a role in the larger whole body differences in energy metabolism in the HCR/LCR that has been described by Britton and Koch et al as the "Energy transfer hypothesis". The hypothesis contends that high vs. low aerobic capacity leads to a greater rate of thermogenesis or metabolic entropy which is supported by evidence that HCR have higher body and skeletal muscle temperature, higher resting energy expenditure, and greater mitochondrial metabolism in skeletal muscle and adipose. Here we tested the hypothesis that reduced intrinsic aerobic capacity and associated reductions in hepatic mitochondrial content, FAO, and MRC would result in increased susceptibility for NASH in the LCR while the high fit-HCR rats who display elevations in these hepatic mitochondrial features would be protected.

Methods

Animals. HCR/LCR rats development and characterization are previously described (Koch & Britton, 2001; Wisloff *et al.*, 2005; Noland *et al.*, 2007; Thyfault *et al.*, 2009; Novak *et al.*, 2010; Gavini *et al.*, 2014; Morris *et al.*, 2014; Vieira-Potter *et al.*, 2015). Male rats (Generation 35) 25-30 weeks of age were singly housed (~75-77°F, 12-hour light cycle) with *ad lib* access to water, and acclimatized to the low-fat, control diet (LFD) (D12110704 (10% kcal fat, 3.5% kcal sucrose, 3.85 kcal/gm), Research Diets, Inc., New Brunswick, NJ, USA) for two weeks prior to the initiation of the western diet (WD) (D09071604 (45% kcal fat, 17% kcal sucrose, 1% cholesterol w/w, 4.68 kcal/gm), Research Diets, Inc.). Food intake and body weight were monitored weekly during the 16 week dietary intervention. Animals were anesthetized with pentobarbital (75 mg/kg, IP) prior to euthanasia via exsanguination and bi-lateral thoracotomy. Tissues were collected and snap frozen in liquid nitrogen after an overnight fast. The animal protocols were approved by the Institutional Animal Care and Use Committee at the University of Missouri and the Subcommittee for Animal Safety at the Harry S Truman Memorial VA Hospital.

Body Composition Analysis. Body composition was measured by magnetic resonance using the EchoMRI-900 analyzer (EchoMRI, Houston, Texas, USA). Body composition was determined before the initiation of WD and periodically throughout the 16 week dietary intervention.

Liver Lipid Analysis. Liver triacylglycerol concentration was determined as previously described using a commercially available kit (Sigma, F6428, St. Louis, MO, USA) (Thyfault *et al.*, 2009). Liver cholesterol was determined utilizing a commercially available kit (Abcam, ab65359, Cambridge, MA, USA).

Liver Histochemical Staining. H&E was performed as described previously (Rector *et al.*, 2010).

Mitochondrial Isolation. Mitochondria were isolated from rat liver tissue, as previously described (Morris *et al.*, 2012). Briefly, tissue was homogenized (Teflon on glass) in cold liver mitochondrial isolation buffer (220 mannitol, 70 sucrose, 10 mM Tris, and 1 mM EDTA, adjusted to pH 7.4 with KOH) and centrifuged (1,500 *g*, 10 min, 4°C). The supernatant was serially centrifuged (8,000 *g* – 6,000 *g* – 4,000 *g*, 10 min, 4°C), with the pellet resuspended (glass on glass) in liver mitochondrial isolation buffer following each centrifugation. The protein concentration was determined by BCA assay.

Mitochondrial Respiration. Mitochondrial oxygen consumption was measured using a Clark type electrode system (Strathkelvin Instruments, North Lanarkshire, Scotland) as previously described (Morris *et al.*, 2013). The consumption of oxygen in nmol/min was normalized to mitochondrial protein in the respirometer cell.

Palmitate Oxidation by Liver Homogenate. The oxidation of [1-^{14}C]-palmitate was measured in fresh liver homogenates as previously described (Morris *et al.*, 2012). Fatty acid oxidation was assessed by measuring the production of $^{14}CO_2$ (complete FAO) and ^{14}C-acid-soluble metabolites in a sealed trapping device at 37°C containing palmitate (200 □M). In order to approximate the CPT-1-mediated and non-CPT-1-mediated FAO in the liver homogenate, parallel incubations were included with the CPT-I inhibitor, etomoxir (100 □M). One animal for each group was analyzed daily. Values were normalized to the wet weight of the liver tissue sample

Pyruvate Oxidation by Isolated Mitochondria. The oxidation of 5 mM pyruvate ([2-^{14}C]-pyruvate) to $^{14}CO_2$ by isolated liver mitochondria was used to monitor pyruvate oxidation and approximate tricarboxylic acid (TCA) cycle flux as previously described (Morris *et al.*, 2012).

Acyl-Carnitine Analysis. Plasma and liver acylcarnitines were measured on an API 3200 triple quadrapole LC-MS/MS as previously described (Satapati *et al.*, 2012). Briefly, liver and plasma free carnitine and acylcarnitines were extracted, derivatized, and individual acylcarnitine peaks were then quantified by comparison with a ^{13}C internal standard (Cambridge Isotopes, Andover, MA). Liver metabolites were normalized to tissue sample weight.

Citrate Synthase Activity. Citrate was determined as previously described (Srere, 1969). Values were normalized to the wet weight of the liver tissue sample.

Liver Nucleotides. Liver ATP, ADP, and AMP were measured by mass spectrometry as described previously (Satapati *et al.*, 2015). Briefly, frozen liver samples were spiked with

[$^{13}C_{10}$, $^{15}N_5$] ATP and [$^{13}C_{10}$, $^{15}N_5$] AMP (Sigma-Aldrich) internal standards before extraction. Analysis was performed on an API 3200 triple quadrupole LC-MS/ MS mass spectrometer (Applied Biosystems/Sciex Instruments) in positive electrospray ionization mode. A reverse-phase C18 column (Waters xBridge, 150 × 2.1 mm, 3 μm) and a gradient elution consisting of water/methanol (5:95, v/v) with 4 mM dibutylamine acetate (eluent A) and acetonitrile with 4 mM dibutylamine acetate (eluent B) was used to achieve separation. Nucleotides were quantified in standard solutions and samples by positive-ion–mode ESI and multiple reaction monitoring (MRM). Liver nucleotides were normalized to tissue sample weight. Liver energy charge was calculated as ([ATP] + ½[ADP]) / ([ATP] + [ADP] + [AMP]).

Western blotting. Triton X-100 cell lysates were used to produce Western blot ready Laemmli samples. Samples were separated by SDS-PAGE, transferred to PVDF membrane and probed with primary antibodies. Bcl-2, Bcl-xL, Bax, Bak, Caspase3, and Caspase 7 antibodies were purchased from Cell Signaling Technologies (Danvers, MA, USA). HADHA antibody was purchased from Abcam (Cambridge, MA, USA). CPT-1a antibody was purchased from Proteintech Group, Inc. (Rosemont, IL, USA). Individual protein bands were quantified using a densitometer (Bio-Rad) and protein loading was corrected by 0.1% amido-black (Sigma) staining to determine total protein as previously described (Morris *et al.*, 2012).

mRNA Expression. RNA and cDNA were prepared as previously described (Morris *et al.*, 2013). Real time quantitative PCR analysis was performed utilizing a Prism 7000 and SYBR green rat primers (listed below). All gene specific values were normalized to relative cyclophilin B mRNA expression values.

Gene	Forward Primer	Reverse Primer
Cyc B	CTTAGCTACAGGAGAGAAAGG	TTCAGCTTGAAGTTCTCCATC
F4/80 (EMR1)	GGAGGACCAATGTTCCAGGG	TGGGCAAGAACAGCTGTAGG
MCP-1 (CCL2)	GAAGCTGTAGTATTTGTCACC	TTCTAATGTACTTCTGGACCC
IL-1B	TAAGCCAACAAGTGGTATTC	AGGTATAGATTCTTCCCCTTG
TLR2	AAAAACTGCTGAGATTTTGC	TACTAACATCCAACACCTCC
TLR4	ACCTAGATCTGAGCTTCAAC	TTGTCTCAATTTCACACCTG
TLR9	AACCTCAGCCATAACATCC	ACTTCCAGCAGTAAGTCTAC
CPT1a	CCTACCACGGCTGGATGTTT	TACAACATGGGCTTCCGACC
HADHA	ACAGGTTTACAAAACAGTGG	CTCTCCAAATTTCTCTGATTCG
HMGCR	GCCTCCATTGACATCCGGAGG	AGGGATGGGAGGCCACAAAG
SOAT1	CTCATATGTCAGAGAGAATGTG	AACTGCATAGCAACATAACC
SOAT2	GGTCAGATTCCTGATGAAAAG	CCACATAATTCCACCTGATG
CES1d	GAGATCCTGACTGAGAAGAG	CTCAGAGATTTTCAGTGTTGG
CES1e	TTCTGCCAACAATGATGAAC	GTTGGTCTTTATTTCTGTCTGG
nCEH1	TGGCCACTGCAAAAAATCAGC	AGGAAGTATTTGGTGGCCCA
CYP7a1	GCGAAGGCATTTGGACACAG	ACCCAGGCATTGCTCTTTGA
CYP17a1	GGCGACAGAAATCTGGTGGA	TGTCCATCAGGCTGGAGATA
HSD17b	AAGAGCTTGCCAAATGGGGA	TCTCTCTCATGACCGGGA
SRD5a1	GTGGTTAGTGGGCATGGTGA	ATTCAAACAGGCCTCCCCTG
ABCG5	CCCTTTGATTTCTACATGGAC	GTTCTTTCAATGTTCTCCAGG
ABCG8	AACAACCTGTGGATAGTACC	GATGGCATAAAGAGGATGTG
ABCA1	GGGAGAGAATGCTGAATATC	CATCTGAAAAACAGGTTTGG
SR-B1 (SCARB1)	CATTCCTTGTTCCTAGACATC	GACGGATTTGATGTACAGAC
LDLR	CAGTGTGAAGATATTGACGAG	TCATCTTACGTACCTCATGG
BSEP (ABCB11)	TGGGGCTCGTCAGATAAGGA	ACATGCGCTGGAGGAAATGA
NTCP (SCL10A1)	CATTCAACTCTGTTCTACCATC	TTTTGTTTGGTCCTTTGC
TGFb	GGAAATCAATGGGATCAGTC	CTGAAGCAGTAGTTGGTATC

COL1a	TGGATTCCAGTTCGAGTATG	AGTGATAGGTGATGTTCTGG
TNFa	CTCACACTCAGATCATCTTC	GAGAACCTGGGAGTAGATAAG
CD11c	CAAAGCTGAGCTGGGAGACA	TGGCTGCTGATGACAGTGTA
CD163	TGTAGTTCATCATCTTCGGTCC	CACCTACCAAGCGGAGTTGAC
CD68	TCACAAAAAGGCTGCCACTCTT	TCGTAGGGCTTCGTTGCTGTGCTT
CD64	GGACAGTGGCGAATACAGGT	CTTCTGTGAGGACTCTGCGG
DR5 (TNFRSF10B)	CATTAGGAAGGAAGTTGCTG	CATTTGGTACAAGACCTCAC
Fas	ATTATAAGCTCCTTTGGCTG	CATCTGAGACATTCATTGGC
TNFRSF1a	CTCCATACATTTGTAGGGATTC	GGAGTTAGGGGCTTAGTAAC
NLRP3	AAGAGGAGTGGATAGGTTTA	CTGTCTTTGATGGAGTAGAAC

Statistical Analysis. Animals within strain were randomized by weight into the two dietary groups. The main effects of phenotype and diet were tested by using 2-way ANOVA SPSS (SPSS Inc., Armonk, NY). Where significant main effects were observed, post hoc analysis was performed using least significant difference to test for any specific pairwise differences. Statistical significance was set at $p<0.05$.

Results

Animal Characteristics. Final body weight was ~16% less in HCR compared to LCR regardless of diet (Table 1, $p<0.05$). However, 16 weeks of WD produced significant weight gain in both HCR and LCR compared to LFD (~60% in each strain, $p<0.05$). The LCR displayed ~20% higher body fat percent than HCR across all diets ($p<0.05$). Interestingly, WD caused no change in body fat percent in the HCR, but caused a ~50% increase in the LCR ($p<0.05$). WD significantly increased liver weight in both HCR and LCR compared to LFD (~2 fold in each strain, $p<0.05$).

Fasting serum and plasma. Circulating glucose and insulin (Table 1) were not different among groups. WD resulted in significant >2-fold increase in AST in both strains and a 2-fold and 4-fold increase in ALT in HCR and LCR, respectively ($p<0.05$), representing a ~60% greater ALT in LCR compared to HCR ($p<0.05$). ALP levels were ~40% lower in LCR rats compared to HCR on LFD ($p<0.05$), and only LCR displayed an increase following WD (67%, $p<0.05$). Finally, the WD diet increased serum cholesterol levels only in the LCR rats

(37%, $p<0.05$). In summary, reduced intrinsic aerobic capacity results in WD-induced increases in body fat and serum markers of liver damage.

Liver histology and lipid analysis. Liver H&E images show increased steatosis in both strains following chronic WD (Figure 1A), however, the LCR displayed greater increases in inflammatory cell infiltration than the HCR following WD feeding. While differences in fiborous markers, TGFb and Col1a1 mRNA expression, were observed due to the WD in both strains (data not shown), no difference was observed in picosirius red staining for fibrosis due to either strain or diet. Unlike previous observations (Thyfault *et al.*, 2009; Morris *et al.*, 2014; Morris *et al.*, 2016), liver triacylglycerol (TAG) content was found to be higher in HCR compared to LCR rats on LFD (Figure 1B, ~35%, $p<0.05$). Chronic WD resulted in a >3.5-fold increase in liver TAG and increases in liver weight in both strains ($p<0.05$). The HCR maintained 38% greater liver TAGs compared to LCR after the WD diet ($p<0.05$). Total liver cholesterol was increased ~3-fold in both strains following WD (Figure 1B, $p<0.05$), and hepatic free cholesterol was increased 67% in HCR and 45% LCR ($p<0.05$). Hepatic cholesterol esters robustly increased in both groups following WD (16- & 29-fold, respectively, $p<0.05$), but was 32% higher in LCR than HCR after WD (interaction, $p<0.05$).

We next examined expression of several genes (i.e. - cholesterol metabolism, bile acid synthesis/steroidogenesis, and cholesterol/bile acid transporters) that may be responsible for strain or diet differences in liver cholesterol ester levels (Table 2). Several genes (e.g. – HMGCR, SOAT2, CYP7a1, HSD17b, & ABCA1) displayed significant changes in expression between the LCR and HCR following chronic WD (significant interactions, $p<0.05$), implicating intrinsic aerobic capacity as a modulator of liver sterol homeostasis. These data show that while HCR and LCR both display WD-induced steatosis, the LCR with reduced intrinsic aerobic capacity are much more susceptible to hepatic cholesterol ester storage and inflammatory cell infiltration.

Liver Inflammation. We next examined hepatic expression of genetic markers of white cell infiltration, recruitment/activation, and initiation/propagation of inflammatory signals. Liver mRNA expression of macrophage marker F4/80 was only increased in the WD-fed LCR (Figure 2A, ~3-fold, interaction, $p<0.05$). In addition, WD resulted in more dramatic increases in MCP-1, IL-1β, and the toll-like receptors 2, 4, and 9 in LCR compared to HCR (Figure 2B&C, significant interactions, $p<0.05$). Hepatic expression of death receptors

TRAIL2, Fas, and TNFR1 were all increased in LCR WD compared to LFD and HCR WD (Figure 2D, $p<0.05$). Furthermore, significant WD-induced increases in liver inflammatory gene expression of NLRP3, TNFa, CD11c, CD68, and CD64 were observed in both strains (Table 2), with no effects of strain observed. These data show that intrinsic aerobic capacity significantly alters susceptibility to WD-induced NASH outcomes.

Liver Fatty Acid Oxidation and Acyl-Carnitine Profiles. We have previously shown that decreased intrinsic aerobic capacity is associated with reduced liver complete fatty acid oxidation (FAO) and more pronounced NAFLD outcomes (Rector *et al.*, 2008; Thyfault *et al.*, 2009; Morris *et al.*, 2012; Morris *et al.*, 2014; Morris *et al.*, 2016). To further assess the role of intrinsic aerobic capacity and chronic WD on liver lipid oxidation, we performed FAO experiments in liver homogenate and determined liver and plasma acyl-carnitine profiles. Chronic WD resulted in a ~45% reduction of complete FAO in both strains (Figure 3A, $p<0.05$), with the HCR WD rats maintaining a 33% greater complete FAO to CO_2 compared to LCR ($p<0.05$). WD resulted in a significant decrease in acid-soluble metabolite (ASM) production in both strains (HCR – 6%, LCR – 18%, $p<0.05$), but a larger decrease in LCR than HCR (interaction, $p<0.05$). These changes were not due to changes in protein expression of CPT-1a, (Figure 3D). However, both complete FAO and ASM production appears to associate with total HADHA protein expression, which was lower in the LCR on LFD and was reduced in both groups by the WD (Figure 3D, $p<0.05$).

While up to 90% of liver FAO is localized to the mitochondria, the impact of increased peroxisomal □-oxidation on liver disease initiation and progression has not been extensively studied. To approximate peroxisomal FAO, liver homogenate FAO was determined in the presence of the CPT-1 inhibitor, etomoxir. In the presences of etomoxir, the relative differences for all FAO data (Figure 3B) strongly mirrored the absolute values above. Complete FAO due to peroxisomal oxidation was ~40% higher in the HCR compared to LCR regardless of diet ($p<0.05$) and ASM production from peroxisomes was also higher in HCR on LFD ($p<0.05$). WD lowered peroxisomal ASM production only in the HCR but not the LCR ($p<0.05$). These data suggest that intrinsic aerobic capacity impacts liver peroxisomal FAO and may impact susceptibility for liver disease.

Acyl-carnitine profiling was performed in liver and plasma to further characterize the role of differing intrinsic aerobic capacity upon lipid metabolism, (Figure 3C & Table 3). WD produced a significant decrease in the C2/C4 acylcarnitine ratio compared to LFD ($p<0.05$) in

both strains due to increases in C4-carnitine. However, the change in C2/C4 was significantly greater following WD in the HCR than the LCR (interaction, $p<0.05$). An opposite effect was observed for the C4/C16 acylcarnitine ratio, where it was increased in both groups following WD, but was increased to a greater extent in the LCR ($p<0.05$). A decrease in the C2/C4 and an increase in the C4/C16 acylcarnitine ratios suggest a decrease in complete fatty acid oxidation and/or an increase in β-oxidation leading to the subsequent accumulation of short-chain C4-carnitine. Additionally, liver long-chain (C14 & C16) acyl-carnitine levels were lower in the LCR compared to HCR, and were lowered in both strains following WD exposures ($p<0.05$). Further, medium-chain (C8) acyl-carnitines were lowered by WD in both strains ($p<0.05$). In addition to implicating increased liver □-oxidation of these species following chronic WD, the lower liver levels of medium- and long-chain acyl-carnitines also may suggest greater diversion of excess liver acyl-CoAs toward the TAG synthesis pathway. This interpretation is supported by the gross steatosis observed in both strains on the WD. Hepatic free carnitine decreased following WD in both strains (Table 3, $p<0.05$), but the reduction was significantly greater in the LCR vs HCR (interaction, $p<0.05$). WD diet caused an equal increase in plasma free carnitine in both strains suggesting that hepatic tissue metabolism following WD was different between strains. Plasma and liver C2-carnitine patterns were similar in the HCR on both diets but the WD significantly decreased liver C2-carnitine in the LCR. All told, these data demonstrate that reduced intrinsic aerobic capacity is associated with decreased hepatic FAO and FAO adaptability to the WD challenge.

Liver Mitochondrial Content, Respiration and Energy State. Reductions in hepatic mitochondrial number, mitochondrial respiratory capacity (MRC), and energy state have also been implicated in the development of NAFLD (Begriche *et al.*, 2013; Arguello *et al.*, 2015). Hepatic mitochondrial content, assessed by citrate synthase activity, was reduced 23% by WD in both strains (Figure 4A, $p<0.05$), however, content remained 16% higher in the HCR than LCR ($p<0.05$). We previously reported (Morris *et al.*, 2014; Morris *et al.*, 2016) evidence of reduced liver mitochondria TCA cycle flux (measured by 2-[14C]-pyruvate oxidation) combined with reduced MRC in LCR. Here we report that WD lowered 2-[14C]-pyruvate oxidation in isolated mitochondria to a greater extent in the LCR vs HCR rats (69% vs 28%, respectively (Figure 4A, $p<0.05$). Similarly, WD feeding reduced ADP-stimulated mitochondrial respiration of glutamate through complex I and complex I&II to a greater extent in LCR vs HCR rats (Figure 4B, $p<0.05$); whereas, maximal uncoupled mitochondrial

respiration of glutamate was significantly increased following WD feeding in HCR compared with LCR (Figure 4B, $p<0.05$). Mitochondrial respiration experiments with pyruvate and palmitoyl-carnitine produced similar findings (data not shown).

Because of differences in hepatic FAO and MRC, we also measured hepatic energy status (NAD and adenine nucleotide pools). LCR displayed greater NADH than HCR on LFD (Table 4, $p<0.05$). WD significantly reduced NAD+, NADH, Total NAD, AMP, ADP, ATP, and total nucleotides in both strains ($p<0.05$). To reduce the impact of WD-induced hepatomegaly on the interpretation of these findings, we calculated within liver sample NAD+/NADH ratio and adenine energy state. Interestingly, no difference due to strain or diet was observed in hepatic energy charge as calculated from adenine nucleotides (Figure 4C). WD significantly lowered NAD+/NADH in both strains ($p<0.05$). Importantly, the greater NADH of the LCR (Table 4) resulted in a lower liver NAD+/NADH ratio compared to HCR on both diets (Figure 4C, $p<0.05$). Chronically reduced NAD+/NADH within the LCR is suggestive of greater oxidative stress (Fisher-Wellman & Neufer, 2012) which was further supported by higher hepatic lipid peroxidation (4-HNE) and evidence of hydrogen peroxide handling (GPx1) in the LCR over HCR (Figure 5, $p<0.05$). In total, these data show that low intrinsic aerobic capacity tracks with reduced liver mitochondrial content, TCA cycle flux, and respiratory capacity that is worsened with a WD. In addition, low-fit LCR rats displayed a more reduced oxidative state, particularly following chronic WD feeding.

Liver Mitochondrial Integrity and Effector Caspase Activation. Mitochondria serve as a primary cellular site for regulation and integration of intra- and extra-cellular signals modulating inflammatory and cell death signaling (Guicciardi *et al.*, 2013). We measured hepatic mitochondrial specific content of Bcl-2 family proteins involved in regulating mitochondrial outer membrane permeability (MOMP) and downstream effector caspases to assess the impact of divergent aerobic capacity and WD on these portions of the cell death cascade. Mitochondrial content of the anti-apoptotic protein Bcl-2 was increased, while Bcl-xL was decreased by WD in both strains (Figure 6A, $p<0.05$). Pro-apoptotic Bcl-2 family members, Bax, Bak, and cleaved Bcl-xL were all significantly increased following WD in both strains (Figure 6B, $p<0.05$). Interestingly, cleaved Bcl-xL mitochondrial localization was greater in LCR rats on both LFD and WD (29% & 39%, respectively) compared to HCR.

To assess whether these elevated markers of mitochondrial outer membrane permeability were associated with activation of downstream pathways, caspase 3 & 7 protein

activation status were determined (Figure 6C). Both caspase 3 & 7 showed greater activation in the LCR compared to HCR regardless of diet (~60% & 4-fold, respectively, $p<0.05$). WD increased activation of caspase 3 but not 7 in HCR and LCR rats (39% & 48%, respectively, $p<0.05$). Thus, WD-induced changes in hepatic mitochondrial integrity between rats with divergent intrinsic aerobic capacities do not result in similarly associated changes in caspase activation. Further, selection for low aerobic capacity is associated with greater basal activation of hepatic effector caspases, which is exacerbated by chronic WD feeding.

Discussion

Despite numerous findings in humans that aerobic capacity impacts liver disease progression mechanisms remain unknown. Likewise, factors that drive transition from NAFLD to NASH in only a portion of patients remains unknown. Herein, we find low aerobic fitness and reduced initial hepatic mitochondrial oxidative capacity enhances susceptibility to WD-induced NASH, as characterized by increased serum ALT, inflammatory cell infiltration, effector caspase activation, and mRNA expression of pro-inflammatory and cell death signaling genes. Importantly, evidence of transition to NASH only occurred in the low fit-LCR despite both high fit-HCR and low fit-LCR developing robust hepatomegaly and steatosis. Overall, the data show that intrinsic aerobic capacity and hepatic mitochondrial oxidative capacity impact cholesterol ester accumulation and inflammatory status following WD, and support the concept that these physiological factors drive risk for transition from NAFLD to NASH.

The roles of both maladaptive liver cholesterol metabolism and hepatic mitochondrial function have been widely investigated in the development of NAFLD (Min *et al.*, 2012; Arguello *et al.*, 2015; Bashiri *et al.*, 2016). Excess dietary cholesterol results in hepatomegaly and steatosis, reduced liver complete and total FAO, and decreased ADP-coupled mitochondrial respiration in rats (Rogers *et al.*, 1980; Fungwe *et al.*, 1993); while chemical inhibition of endogenous cholesterol synthesis increased hepatic mitochondrial and peroxisomal FAO with protection from NASH development (Roglans *et al.*, 2002; Park *et al.*, 2016). In the current study, WD reduced FAO (complete and incomplete) and MRC in both strains, but the LCR started at a lower level and remained lower than HCR rats. In addition, the impact of the lower levels of FAO and MRC in isolated mitochondria is further magnified by the overall lower mitochondrial content in the LCR vs. HCR rats. Similar findings were observed with markers of liver mitochondrial content, TCA cycle flux, and free hepatic

carnitine content. We have previously observed that LCR rats have increased susceptibility to steatosis, which was associated with reduced whole body FAO, metabolic inflexibility, decreased liver FAO, and reduced MRC (Thyfault *et al.*, 2009; Morris *et al.*, 2014; Morris *et al.*, 2016). These data are similar to human NAFLD subjects who have been shown to have physiological features that include lower aerobic capacity, metabolic inflexibility, decreased whole body FAO, and reduced □-hydroxybutyrate, all factors that suggest reduced liver FAO capacity (Croci *et al.*, 2012). Additional rodent studies have demonstrated that reduced hepatic complete FAO is associated with development and progression of hepatic steatosis (Rector *et al.*, 2008; Rector *et al.*, 2010) while molecular therapies to enhance FAO effectively treat or prevent steatosis. Importantly, our findings of greater WD-induced reductions in mitochondrial FAO and MRC in LCR rats appear to be independent of TAG accumulation. Suggesting that hepatic TAG stores are not the primary driver of inflammation and oxidative stress, but rather that hepatic mitochondrial function plays a more important role. These results are similar to the athletes' paradox by which both athletes and insulin resistant obese individuals display dramatically different insulin sensitivity and inflammation despite both displaying elevated intramuscular lipids (Goodpaster *et al.*, 2001). Much like in muscle, it is the possible that the overall balance of hepatic mitochondrial content/oxidative capacity and lipid stores interact to impact outcomes related to inflammation and insulin resistance.

Mitochondria are hypothesized to serve as a cellular point of integration of intra- and extra-cellular signals ultimately producing inflammation and cell death signaling (Guicciardi *et al.*, 2013; Luedde *et al.*, 2014; Arguello *et al.*, 2015). Dysregulated liver cholesterol homeostasis and accumulation have been implicated in the initiation of hepatic mitochondrial dysfunction (Montero *et al.*, 2010), which is associated with NAFLD severity (Min *et al.*, 2012). Mitochondrion membranes are inherently cholesterol poor (Montero *et al.*, 2010), with increased mitochondrial membrane cholesterol producing decreased ATP synthesis (Campbell & Chan, 2007) and decreased mitochondrial antioxidant capacity (Fernandez-Checa & Kaplowitz, 2005). In the present study, maximal ADP-coupled MRC was lowered to a greater extent following WD in the LCR rats, results that tracked with greater induction of mitochondrial oxidative stress. Previously, increased free cholesterol levels were highly associated with NASH-related mitochondrial dysfunction (Min *et al.*, 2012; Gan *et al.*, 2014). Interestingly, here the reductions in MRC and increased markers of oxidative stress occurred in parallel with an observed increase in cholesterol ester in LCR compared to HCR on the

WD. Chronic accumulation of mitochondrial cholesterol is associated with increased mitochondrial localization of pro-apoptotic Bcl-2 family members and activation of mitochondrial out membrane permeability (MOMP) (Montero *et al.*, 2010). Chronic WD feeding in this study resulted in similar increases in mitochondrial protein localization of Bax and Bak in both strains, while lowering the predominant liver anti-MOMP Bcl family member, Bcl-xL. Mitochondrial localization of the pro-apoptotic Bcl-xL cleavage product (Clem *et al.*, 1998; Fujita *et al.*, 1998) was significantly higher in the WD fed LCR rats compared to HCR, and was strongly associated with the observed increases in markers of advance NAFLD.

We found that effector caspase activation was higher in LCR rats compared to HCR regardless of diet, with WD dramatically increasing caspase-3 activation further. This increase in caspase-3 activation could potentially explain the observed increase in cleaved Bcl-xL (Clem *et al.*, 1998; Fujita *et al.*, 1998). The increased effector caspase activation also suggests greater intrinsic/extrinsic cell death signaling in the LCR on WD which is further supported by the observed increases in cell death receptor expression. As mentioned, there is considerable evidence that loss of mitochondrial function and excess cholesterol can result in propagation of these intrinsic/extrinsic cell death signals (Guicciardi *et al.*, 2013; Luedde *et al.*, 2014; Arguello *et al.*, 2015). However, any increased cell death signaling in the LCR rats on WD is early in the disease process as assessment of cell death by TUNEL assay showed no differences between HCR and LCR rats (data not shown). Together, these data suggest that intrinsically low aerobic capacity results in increased susceptibility to WD-induced steatohepatitis due to lower mitochondrial respiratory capacity, increased oxidative stress, and greater activation of effector caspases.

In summary, we demonstrate that intrinsic aerobic capacity impacts susceptibility for WD-induced NASH. Lower initial levels and further declines in liver FAO, and MRC, paired with excessive liver cholesterol ester accumulation lead to greater increases in several markers of liver damage and inflammation in the low fit-LCR compared to the high fit-HCR rats. Of note, while high intrinsic aerobic capacity HCR rats were less susceptible to many of the liver mal-adaptations induced by a WD, HCR rats were not completely protective against hepatomegaly/liver TAG accumulation or against a loss of mitochondrial-FAO or MRC unlike our previous findings with acute and chronic high-fat diets (Thyfault *et al.*, 2009;

Morris *et al.*, 2014; Morris *et al.*, 2016). These data support a novel concept that aerobic capacity and hepatic mitochondrial phenotype may play a critical role in whether NAFLD transitions to NASH, links that require further examination in human patients. Overall, these data provide new insight into how intrinsic aerobic capacity may influence the onset and progression of metabolic disease through hepatic mitochondrial oxidative capacity.

GRANTS and ACKNOLDGEMENTS

This work was partially supported by NIH DK088940 (JPT), NIH 5T32AR48523-8 (EMM), AHA 14POST20110034 (EMM), VHA-CDA2 IK2BX001299 (RSR), and VA Merit Review; 1I01BX002567-01(JPT), NIH RO1DK078184 (SCB), and the Robert A. Welch Foundation I-1804 (SCB). This work was supported with resources and the use of facilities at the Harry S Truman Memorial VA Hospital in Columbia, MO. The LCR-HCR rat model system was funded by the Office of Research Infrastructure Programs grant P40OD021331 (LGK and SLB) from the National Institutes of Health. We acknowledge the expert care of the rat colony provided by Molly Kalahar and Lori Heckenkamp. Contact LGK lgkoch@umich.edu or SLB brittons@umich.edu for information on the LCR and HCR rats: these rat models are maintained as an international resource with support from the Department of Anesthesiology at the University of Michigan, Ann Arbor, Michigan.

Disclosures

The authors have no conflicts of interest to disclose for this research.

Bibliography

Arguello G, Balboa E, Arrese M & Zanlungo S. (2015). Recent insights on the role of cholesterol in non-alcoholic fatty liver disease. *Biochim Biophys Acta* **1852,** 1765-1778.

Bashiri A, Nesan D, Tavallaee G, Sue-Chue-Lam I, Chien K, Maguire GF, Naples M, Zhang J, Magomedova L, Adeli K, Cummins CL & Ng DS. (2016). Cellular cholesterol accumulation modulates high fat high sucrose (HFHS) diet-induced ER stress and hepatic inflammasome activation in the development of non-alcoholic steatohepatitis. *Biochim Biophys Acta* **1861,** 594-605.

Begriche K, Massart J, Robin MA, Bonnet F & Fromenty B. (2013). Mitochondrial adaptations and dysfunctions in nonalcoholic fatty liver disease. *Hepatology* **58,** 1497-1507.

Bernal W, Martin-Mateos R, Lipcsey M, Tallis C, Woodsford K, McPhail MJ, Willars C, Auzinger G, Sizer E, Heneghan M, Cottam S, Heaton N & Wendon J. (2014). Aerobic capacity during cardiopulmonary exercise testing and survival with and without liver transplantation for patients with chronic liver disease. *Liver Transpl* **20,** 54-62.

Campbell AM & Chan SH. (2007). The voltage dependent anion channel affects mitochondrial cholesterol distribution and function. *Arch Biochem Biophys* **466,** 203-210.

Church TS, Kuk JL, Ross R, Priest EL, Biltoft E & Blair SN. (2006). Association of cardiorespiratory fitness, body mass index, and waist circumference to nonalcoholic fatty liver disease. *Gastroenterology* **130,** 2023-2030.

Clem RJ, Cheng EH, Karp CL, Kirsch DG, Ueno K, Takahashi A, Kastan MB, Griffin DE, Earnshaw WC, Veliuona MA & Hardwick JM. (1998). Modulation of cell death by Bcl-XL through caspase interaction. *Proc Natl Acad Sci U S A* **95,** 554-559.

Croci I, Byrne NM, Choquette S, Hills AP, Chachay VS, Clouston AD, O'Moore-Sullivan TM, Macdonald GA, Prins JB & Hickman IJ. (2012). Whole-body substrate metabolism is associated with disease severity in patients with non-alcoholic fatty liver disease. *Gut*.

Fernandez-Checa JC & Kaplowitz N. (2005). Hepatic mitochondrial glutathione: transport and role in disease and toxicity. *Toxicol Appl Pharmacol* **204,** 263-273.

Fisher-Wellman KH & Neufer PD. (2012). Linking mitochondrial bioenergetics to insulin resistance via redox biology. *Trends in endocrinology and metabolism: TEM* **23,** 142-153.

Fujita N, Nagahashi A, Nagashima K, Rokudai S & Tsuruo T. (1998). Acceleration of apoptotic cell death after the cleavage of Bcl-XL protein by caspase-3-like proteases. *Oncogene* **17,** 1295-1304.

Fungwe TV, Cagen LM, Cook GA, Wilcox HG & Heimberg M. (1993). Dietary cholesterol stimulates hepatic biosynthesis of triglyceride and reduces oxidation of fatty acids in the rat. *J Lipid Res* **34,** 933-941.

Gan LT, Van Rooyen DM, Koina ME, McCuskey RS, Teoh NC & Farrell GC. (2014). Hepatocyte free cholesterol lipotoxicity results from JNK1-mediated mitochondrial injury and is HMGB1 and TLR4-dependent. *J Hepatol* **61,** 1376-1384.

Gavini CK, Mukherjee S, Shukla C, Britton SL, Koch LG, Shi H & Novak CM. (2014). Leanness and Heightened Non-Resting Energy Expenditure: Role of Skeletal Muscle Activity Thermogenesis. *Am J Physiol Endocrinol Metab*.

Goodpaster BH, He J, Watkins S & Kelley DE. (2001). Skeletal muscle lipid content and insulin resistance: evidence for a paradox in endurance-trained athletes. *J Clin Endocrinol Metab* **86,** 5755-5761.

Guicciardi ME, Malhi H, Mott JL & Gores GJ. (2013). Apoptosis and necrosis in the liver. *Compr Physiol* **3,** 977-1010.

Kantartzis K, Thamer C, Peter A, Machann J, Schick F, Schraml C, Konigsrainer A, Konigsrainer I, Krober S, Niess A, Fritsche A, Haring HU & Stefan N. (2009). High cardiorespiratory fitness is an independent predictor of the reduction in liver fat during a lifestyle intervention in non-alcoholic fatty liver disease. *Gut* **58,** 1281-1288.

Koch LG & Britton SL. (2001). Artificial selection for intrinsic aerobic endurance running capacity in rats. *Physiol Genomics* **5,** 45-52.

Linden MA, Sheldon RD, Meers GM, Ortinau LC, Morris EM, Booth FW, Kanaley JA, Vieira-Potter VJ, Sowers JR, Ibdah JA, Thyfault JP, Laughlin MH & Rector RS. (2016). Aerobic exercise training in the treatment of NAFLD related fibrosis. *J Physiol*.

Luedde T, Kaplowitz N & Schwabe RF. (2014). Cell death and cell death responses in liver disease: mechanisms and clinical relevance. *Gastroenterology* **147,** 765-783 e764.

Matteoni CA, Younossi ZM, Gramlich T, Boparai N, Liu YC & McCullough AJ. (1999). Nonalcoholic fatty liver disease: a spectrum of clinical and pathological severity. *Gastroenterology* **116,** 1413-1419.

Min HK, Kapoor A, Fuchs M, Mirshahi F, Zhou H, Maher J, Kellum J, Warnick R, Contos MJ & Sanyal AJ. (2012). Increased hepatic synthesis and dysregulation of cholesterol metabolism is associated with the severity of nonalcoholic fatty liver disease. *Cell Metab* **15,** 665-674.

Montero J, Mari M, Colell A, Morales A, Basanez G, Garcia-Ruiz C & Fernandez-Checa JC. (2010). Cholesterol and peroxidized cardiolipin in mitochondrial membrane properties, permeabilization and cell death. *Biochim Biophys Acta* **1797,** 1217-1224.

Morris EM, Jackman MR, Johnson GC, Liu TW, Lopez JL, Kearney ML, Fletcher JA, Meers GM, Koch LG, Britton SL, Rector RS, Ibdah JA, MacLean PS & Thyfault JP. (2014). Intrinsic aerobic capacity impacts susceptibility to acute high-fat diet-induced hepatic steatosis. *Am J Physiol Endocrinol Metab* **307,** E355-364.

Morris EM, Jackman MR, Meers GM, Johnson GC, Lopez JL, Maclean PS & Thyfault JP. (2013). Reduced hepatic mitochondrial respiration following acute high-fat diet is prevented by PGC-1alpha overexpression. *Am J Physiol Gastrointest Liver Physiol* **305,** G868-880.

Morris EM, Meers GM, Booth FW, Fritsche KL, Hardin CD, Thyfault JP & Ibdah JA. (2012). PGC-1alpha overexpression results in increased hepatic fatty acid oxidation with reduced triacylglycerol accumulation and secretion. *Am J Physiol Gastrointest Liver Physiol* **303,** G979-992.

Morris EM, Meers GM, Koch LG, Britton SL, Fletcher JA, Shankar K, Fu X, Burgess SC, Ibdah JA, Rector RS & Thyfault JP. (2016). Aerobic capacity and hepatic mitochondrial lipid oxidation alters susceptibility for chronic high fat diet induced hepatic steatosis. *Am J Physiol Endocrinol Metab***,** ajpendo 00178 02016.

Musso G, Gambino R, De Michieli F, Cassader M, Rizzetto M, Durazzo M, Faga E, Silli B & Pagano G. (2003). Dietary habits and their relations to insulin resistance and postprandial lipemia in nonalcoholic steatohepatitis. *Hepatology* **37,** 909-916.

Myers J, Prakash M, Froelicher V, Do D, Partington S & Atwood JE. (2002). Exercise capacity and mortality among men referred for exercise testing. *N Engl J Med* **346,** 793-801.

Noland RC, Thyfault JP, Henes ST, Whitfield BR, Woodlief TL, Evans JR, Lust JA, Britton SL, Koch LG, Dudek RW, Dohm GL, Cortright RN & Lust RM. (2007). Artificial selection for high-capacity endurance running is protective against high-fat diet-induced insulin resistance. *Am J Physiol Endocrinol Metab* **293,** E31-41.

Novak CM, Escande C, Burghardt PR, Zhang M, Barbosa MT, Chini EN, Britton SL, Koch LG, Akil H & Levine JA. (2010). Spontaneous activity, economy of activity, and resistance to diet-induced obesity in rats bred for high intrinsic aerobic capacity. *Horm Behav* **58,** 355-367.

Park HS, Jang JE, Ko MS, Woo SH, Kim BJ, Kim HS, Park HS, Park IS, Koh EH & Lee KU. (2016). Statins Increase Mitochondrial and Peroxisomal Fatty Acid Oxidation in the Liver and Prevent Non-Alcoholic Steatohepatitis in Mice. *Diabetes Metab J*.

Rector RS, Thyfault JP, Morris RT, Laye MJ, Borengasser SJ, Booth FW & Ibdah JA. (2008). Daily exercise increases hepatic fatty acid oxidation and prevents steatosis in Otsuka Long-Evans Tokushima Fatty rats. *Am J Physiol Gastrointest Liver Physiol* **294,** G619-626.

Rector RS, Thyfault JP, Uptergrove GM, Morris EM, Naples SP, Borengasser SJ, Mikus CR, Laye MJ, Laughlin MH, Booth FW & Ibdah JA. (2010). Mitochondrial dysfunction precedes insulin resistance and hepatic steatosis and contributes to the natural history of non-alcoholic fatty liver disease in an obese rodent model. *J Hepatol* **52,** 727-736.

Ren YY, Overmyer KA, Qi NR, Treutelaar MK, Heckenkamp L, Kalahar M, Koch LG, Britton SL, Burant CF & Li JZ. (2013). Genetic analysis of a rat model of aerobic capacity and metabolic fitness. *PLoS One* **8,** e77588.

Rogers KS, Higgins ES & Grogan WM. (1980). Influence of dietary cholesterol on mitochondrial function in the rat. *The Journal of nutrition* **110,** 248-254.

Roglans N, Sanguino E, Peris C, Alegret M, Vazquez M, Adzet T, Diaz C, Hernandez G, Laguna JC & Sanchez RM. (2002). Atorvastatin treatment induced peroxisome proliferator-activated receptor alpha expression and decreased plasma nonesterified fatty acids and liver triglyceride in fructose-fed rats. *J Pharmacol Exp Ther* **302,** 232-239.

Satapati S, Kucejova B, Duarte JA, Fletcher JA, Reynolds L, Sunny NE, He T, Nair LA, Livingston K, Fu X, Merritt ME, Sherry AD, Malloy CR, Shelton JM, Lambert J, Parks EJ, Corbin I, Magnuson MA, Browning JD & Burgess SC. (2015). Mitochondrial metabolism mediates oxidative stress and inflammation in fatty liver. *J Clin Invest* **125,** 4447-4462.

Satapati S, Sunny NE, Kucejova B, Fu X, He TT, Mendez-Lucas A, Shelton JM, Perales JC, Browning JD & Burgess SC. (2012). Elevated TCA cycle function in the pathology of diet-induced hepatic insulin resistance and fatty liver. *J Lipid Res* **53,** 1080-1092.

Srere PA. (1969). Citrate Synthase. *Methods Enzymol* **13,** 3-11.

Thyfault JP, Rector RS, Uptergrove GM, Borengasser SJ, Morris EM, Wei Y, Laye MJ, Burant CF, Qi NR, Ridenhour SE, Koch LG, Britton SL & Ibdah JA. (2009). Rats selectively bred for low aerobic capacity have reduced hepatic mitochondrial oxidative capacity and susceptibility to hepatic steatosis and injury. *J Physiol* **587,** 1805-1816.

Vieira-Potter VJ, Padilla J, Park YM, Welly RJ, Scroggins RJ, Britton SL, Koch LG, Jenkins NT, Crissey JM, Zidon T, Morris EM, Meers GM & Thyfault JP. (2015). Female rats selectively bred for high intrinsic aerobic fitness are protected from ovariectomy-associated metabolic dysfunction. *Am J Physiol Regul Integr Comp Physiol* **308,** R530-542.

Wisloff U, Najjar SM, Ellingsen O, Haram PM, Swoap S, Al-Share Q, Fernstrom M, Rezaei K, Lee SJ, Koch LG & Britton SL. (2005). Cardiovascular risk factors emerge after artificial selection for low aerobic capacity. *Science* **307,** 418-420.

Table 1 – Animal Characteristics. Final body weight, total weight gain, percent body fat, percent body fat change after the 16 weeks WD are expressed as means ± SEM (n=8). Average weekly energy intake during the 16 week WD are expressed as means ± SEM (n=8). Weekly feed efficiency as weekly body weight gain divided by weekly energy intake is expressed as means ± SEM (n=8). Liver weight in grams is expressed as means ± SEM (n=8). Fasting serum alanine transaminase (ALT), aspartate aminotransferase (AST), alkaline phosphatase (ALP), cholesterol following the 16 weeks WD are expressed as means ± SEM (n=8). Fasting plasma glucose and insulin following the 16 weeks WD are expressed as means ± SEM (n=8). * $p<0.05$ main effect HCR vs. LCR, † $p<0.05$ main effect LFD vs. WD, ** $p<0.05$ HCR vs. LCR within diet, †† $p<0.05$ LFD vs. WD within strain.

	HCR		LCR	
	LFD	**WD**	**LFD**	**WD**
Anthropometrics				
Body Weight (g)	436.9 ± 23.6	460.5 ± 19.2	511.6 ± 29.5*	560.8 ± 32.8*
Weight Gain (g)	50.8 ± 6.9	82.7 ± 9.7†	34.1 ± 7.1	88.9 ± 14.2†
Body Fat %	19.3 ± 1.5	21.6 ± 1.5	24.6 ± 1.7*	26.8 ± 1.5*
Change in Body Fat %	5.5 ± 1.2	6.3 ± 0.8	6.9 ± 0.9	10.2 ± 0.4**,††
Energy Intake (weekly average - kcal)	387.8 ± 15.5	431.5 ± 10.6††	394.7 ± 22.3	424.9 ± 18.9
Feed Efficiency (weekly average - mg/kcal)	9.3 ± 1.4	11.4 ± 1.4	6.4 ± 1.5	11.9 ± 1.4††
Liver Weight (g)	9.2 ± 0.5	18.2 ± 1.2†	9.9 ± 0.6	17.6 ± 1.4†
Serum				
ALT (U/L)	45.4 ± 4.2	126.1 ± 25.6†	51.6 ± 9.9	206.1 ± 30.6†,**
AST (U/L)	99.8 ± 10.2	196.6 ± 38.1†	96.3 ± 11.5	238.9 ± 29.0†
ALP (U/L)	118.0 ± 6.4	133.4 ± 10.2	71.0 ± 4.5**	118.3 ± 6.1††
Cholesterol (mg/dL)	86.1 ± 6.4	92.1 ± 16.7	98.1 ± 7.9	134.0 ± 8.6**,††
Plasma				
Glucose (mg/dL)	169.1 ± 8.5	174.5 ± 7.4	172.5 ± 9.9	167.9 ± 5.1
Insulin (ng/mL)	1.39 ± 0.18	1.47 ± 0.19	1.08 ± 0.17	1.37 ± 0.21

Table 2 – Liver Bile Acid Metabolism and Inflammation Death mRNA Expression. Gene expression in liver was determined by RT-PCR. Relative expression of listed genes related to liver bile acid metabolism and inflammation state were normalized to cyclophilin B (PPIB) and presented as means ± SEM (n=7-8). * p<0.05 main effect HCR vs. LCR, † p<0.05 main effect LFD vs. WD, ** p<0.05 HCR vs. LCR within diet, †† p<0.05 LFD vs. WD within strain.

	HCR		**LCR**		
	LFD	**WD**	**LFD**	**WD**	**Interaction**
Cholesterol Ester Metabolism					
HMGCR	1.01 ± 0.06	0.60 ± 0.06††	0.47 ± 0.04*	0.43 ± 0.05*	p<0.002
SOAT1	1.03 ± 0.11	3.25 ± 0.71†	0.94 ± 0.08	2.69 ± 0.45†	NS
SOAT2	1.01 ± 0.04	0.62 ± 0.04††	0.87 ± 0.07*	0.89 ± 0.03*	p<0.001
nCEH1	1.01 ± 0.06	1.19 ± 0.11	1.82 ± 0.21*	1.80 ± 0.18*	NS
CES1d	1.07 ± 0.14	1.33 ± 0.29	0.93 ± 0.10	1.04 ± 0.17	NS
CES1e	1.00 ± 0.04	0.96 ± 0.11	1.23 ± 0.08*	1.12 ± 0.12*	NS
Bile Acid /Steroidogenesis					
CYP7a1	1.10 ± 0.17	1.44 ± 0.15	0.44 ± 0.07*	3.80 ± 0.64*,††	p<0.0001
CYP17a1	1.08 ± 0.26	0.41 ± 0.08††	0.98 ± 0.21	0.85 ± 0.25	NS
HSD17b	0.93 ± 0.13	0.58 ± 0.09††	1.51 ± 0.26*	2.65 ± 0.47*,††	p<0.02
SRD5a1	1.05 ± 0.13	0.30 ± 0.03	0.83 ± 0.8	0.31 ± 0.11	NS
Cholesterol/Bile Transporters					

ABCG5	1.08 ± 0.16	1.86 ± 0.35††	0.74 ± 0.14	0.92 ± 0.17**	NS
ABCG8	1.07 ± 0.16	0.60 ± 0.17†	2.65 ± 0.53*	1.26 ± 0.23*,†	NS
ABCA1	1.02 ± 0.08	1.18 ± 0.06	1.00 ± 0.11	1.64 ± 0.15**,††	p<0.05
SR-B1 (SCARB1)	1.03 ± 0.09	0.80 ± 0.05††	1.06 ± 0.07	1.04 ± 0.08**	NS
LDLR	1.03 ± 0.09	0.35 ± 0.06†	0.91 ± 0.06	0.41 ± 0.02†	NS
BSEP (ABCB11)	1.01 ± 0.05	0.88 ± 0.07†	1.33 ± 0.05*	1.03 ± 0.10*,†	NS
NTCP (SCL10A1)	1.01 ± 0.05	0.52 ± 0.06†	1.03 ± 0.10	0.70 ± 0.07†	NS
Inflammation					
NLRP3	1.09 ± 0.18	2.38 ± 0.41†	0.87 ± 0.08	2.81 ± 0.33†	NS
TNFa	0.94 ± 0.11	3.39 ± 0.60†	0.69 ± 0.08	5.26 ± 1.33†	NS
CD11c	1.00 ± 0.06	3.27 ± 0.46†	0.78 ± 0.12	4.04 ± 0.67†	NS
CD68	1.08 ± 0.15	2.38 ± 0.40†	0.81 ± 0.06	2.56 ± 0.36†	NS
CD64	0.94 ± 0.11	1.59 ± 0.20†	0.83 ± 0.07	1.89 ± 0.25†	NS

Table 3 – Plasma and Liver Acyl-Carnitine Profiles. Plasma and liver acyl-carnitines were quantitated by LC-MS/MS. Liver acyl-carnitines were normalized to liver samples weight. All values are presented as means ± SEM (n=7-8). $p<0.05$ interaction, * $p<0.05$ main effect HCR vs. LCR, † $p<0.05$ main effect LFD vs. WD, ** $p<0.05$ HCR vs. LCR within diet, †† $p<0.05$ LFD vs. WD within strain.

	HCR		LCR		
	LFD	**WD**	**LFD**	**WD**	**Interaction**
Serum (□M)					
Free Carnitine	40.64 ± 2.85	49.87 ± 2.49††	55.31 ± 2.64*	57.93 ± 2.38*	NS
Acetyl-Carnitine (C2)	27.77 ± 2.26	29.88 ± 1.58	39.63 ± 3.07*	36.53 ± 2.21*	NS
Isopropyl-Carnitine (C3)	0.1532 ± 0.0150	0.2467 ± 0.0122†	0.2207 ± 0.0143*	0.3662 ± 0.0132*,†	p<0.07
Butyryl-Carnitine (C4)	0.2962 ± 0.0245	0.3218 ± 0.0463	0.4153 ± 0.0195*	0.4610 ± 0.0492*	NS
Isovaleryl-Carnitine (C5)	0.0112 ± 0.0021	0.0107 ± 0.0003	0.0113 ± 0.0007	0.0127 ± 0.0006	NS
Octanoyl-Carnitine (C8)	0.0139 ± 0.0007	0.0126 ± 0.0004	0.0134 ± 0.0004	0.0137 ± 0.0006	NS
Mistroyl-Carnitine (C14)	0.0546 ± 0.0041	0.0491 ± 0.0038	0.0555 ± 0.0027	0.0424 ± 0.0017††	NS
Palmitoyl-Carnitine (C16)	0.3358 ± 0.0488	0.3361 ± 0.0400	0.3652 ± 0.0267	0.3138 ± 0.0215	NS
Liver (nmol/g)					
Free Carnitine	304.2 ± 10.9	209.3 ± 23.2†	335.9 ± 7.2*	123.6 ± 7.9*,†	p<0.001
Acetyl-Carnitine (C2)	105.7 ± 10.2	109.3 ± 9	99.4 ± 11.2	110.3 ± 8.2	NS
Isopropyl-Carnitine (C3)	3.22 ± 0.74	3.91 ± 0.36	1.72 ± 0.18**	3.09 ± 0.36††	NS
Butyryl-Carnitine (C4)	0.650 ± 0.230	3.119 ± 0.611†	1.315 ± 0.362	5.048 ± 1.370†	NS
Isovaleryl-Carnitine (C5)	0.1321 ± 0.0190	0.1566 ± 0.217	0.1434 ± 0.0123	0.1052 ± 0.181	NS

Octanoyl-Carnitine (C8)	0.0592 ± 0.0106	0.0226 ± 0.0052†	0.0555 ± 0.0110	0.0151 ± 0.0014†	NS
Mistroyl-Carnitine (C14)	1.250 ± 0.232	0.216 ± 0.061†	0.676 ± 0.142**	0.213 ± 0.049†	p<0.07
Palmitoyl-Carnitine (C16)	1.185 ± 0.187	0.490 ± 0.133†	0.671 ± 0.136*	0.266 ± 0.030*,†	NS
Liver Carnitine Ratios					
C2/C3	48.4 ± 7.9	29.2 ± 3.2†	52.8 ± 4.6	37.5 ± 2.9†	NS
C2/C4	285.2 ± 65.0	44.5 ± 9.6†	110.3 ± 33.1*	30.3 ± 5.0*,†	p<0.05
C4/C16	0.312 ± 0.078	7.480 ± 2.022†	2.929 ± 1.230*	14.276 ± 2.894*,†	NS
C8/C16	0.039 ± 0.006	0.033 ± 0.004	0.091 ± 0.012*	0.066 ± 0.007*,††	NS

Table 4 – Liver Adenine Nucleotides. Chronic high-fat/high-cholesterol diet lowers liver adenine nucleotides in HCR/LCR rats. Liver adenine nucleotide (NAD+, NADH, AMP, ADP, and ATP) quantitation was determined by LC-MS/MS and all values were normalized to liver sample weight. All values are presented as means ± SEM (n=7-8). $p<0.05$ interaction, * $p<0.05$ main effect HCR vs. LCR, † $p<0.05$ main effect LFD vs. WD, ** $p<0.05$ HCR vs. LCR within diet, †† $p<0.05$ LFD vs. WD within strain.

	HCR		**LCR**		
	LFD	**WD**	**LFD**	**WD**	**Interaction**
NAD Pool (nmol/g)					
NAD^+	1022.6 ± 40.3	641.0 ± 31.3†	1078.4 ± 84.6	553.0 ± 44.7†	NS
NADH	158.8 ± 10.0	130.6 ± 8.1†	239.7 ± 28.6*	158.4 ± 9.2*,†	p=0.06
Total NAD	1181.5 ± 38.1	783.9 ± 40.4†	1318.1 ± 101.7*	711.3 ± 42.9*,†	p=0.06
Adenine Nucleotide Pool (nmol/g)					
AMP	855.2 ± 42.4	663.9 ± 72.4†	938.1 ± 64.9	581.8 ± 70.6†	NS

ADP	1549.7 ± 90.2	1220.7 ± 101.9†	1863.9 ± 137.7	1186.2 ± 111.7†	NS
ATP	2254.2 ± 76.2	1553.7 ± 82.3†	2467.0 ± 117.6	1739.8 ± 180.6†	NS
Total Adenine Pool	4659.1 ± 124.8	3438.3 ± 217.5†	5429.2 ± 376.8	3507.8 ± 242.5†	NS

Figure 1 – High intrinsic aerobic capacity protects against high-fat/high-cholesterol diet-induced hepatic steatosis and non-parenchymal cellular infiltration. Representative H&E images (20X) are presented in Figure 2A. Liver triacylglycerol (Figure 2B), total cholesterol, free cholesterol, and cholesterol ester were determined biochemically. Values are means ± SEM (n=8). § $p<0.05$ interaction, * $p<0.05$ main effect HCR vs. LCR, † $p<0.05$ main effect LFD vs. WD.

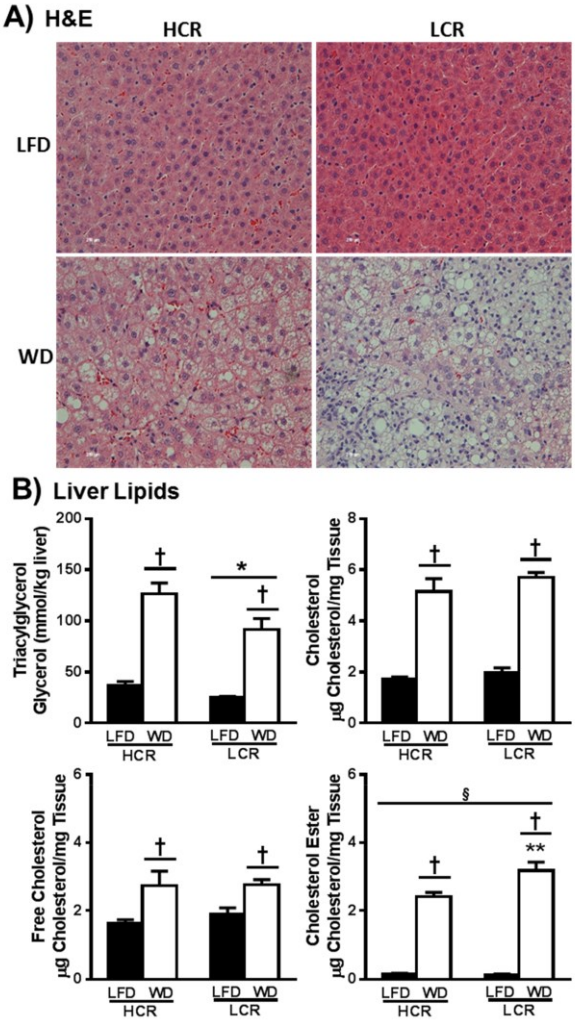

Figure 2 – High intrinsic aerobic capacity attenuates high-fat/high-cholesterol diet-induced expression of markers of liver macrophage infiltration and inflammation. Gene expression in liver was determined by RT-PCR. Relative mRNA expression of genes for (A) macrophage markers, (B) recruitment and activation, (C) inflammation initiation & propagation, and (D) death receptors were normalized to cyclophilin B (PPIB) and presented as means ± SEM (n=7-8). § $p<0.05$ interaction, * $p<0.05$ main effect HCR vs. LCR, † $p<0.05$ main effect LFD vs. WD, ** $p<0.05$ HCR vs. LCR within diet.

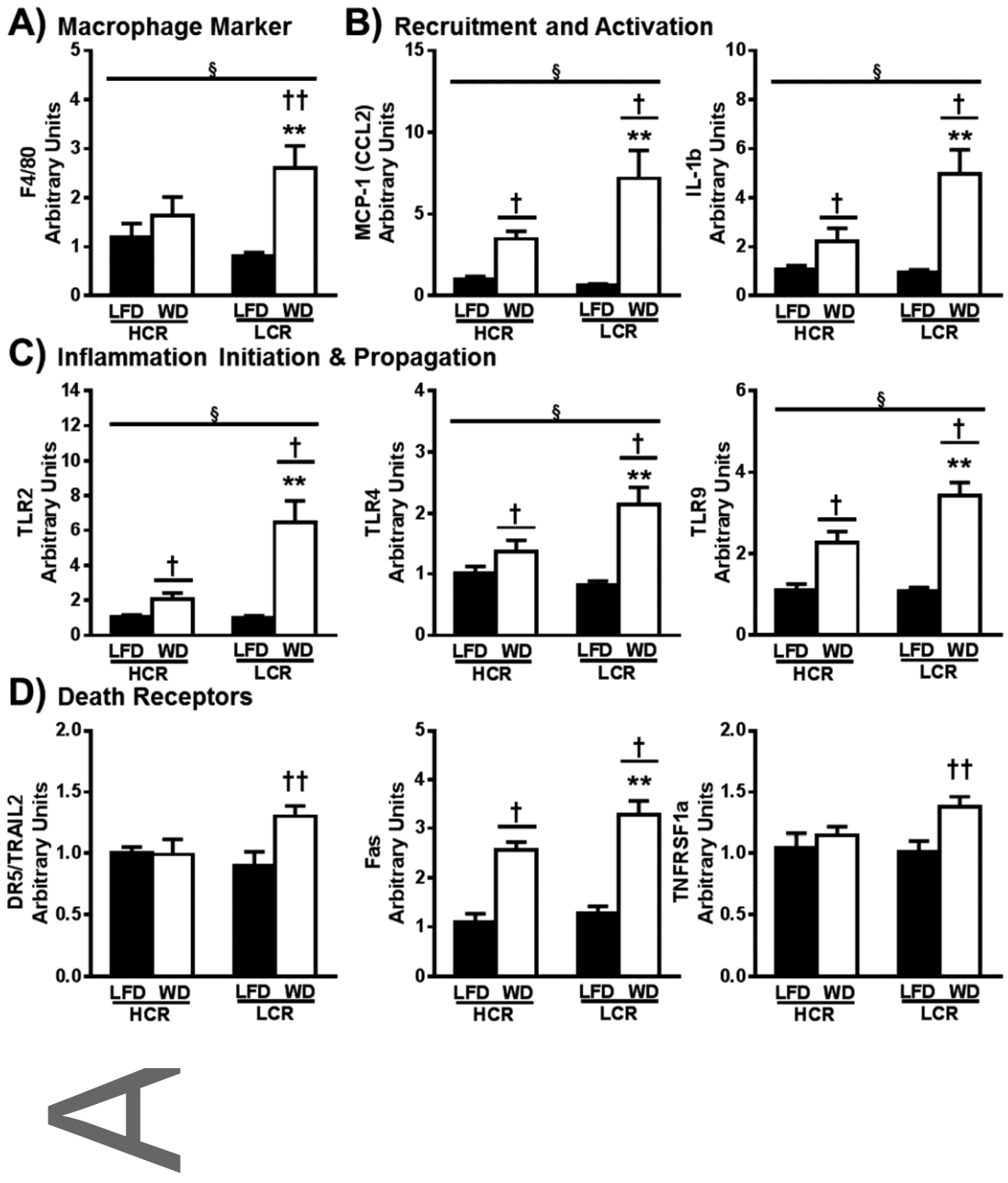

Figure 3 – Selection for increased running capacity results in greater hepatic fatty acid oxidation (FAO) and acyl-carnitine flux. Liver homogenates were incubated with ^{14}C-palmitate. Complete FAO (A) was determined by trapping $^{14}CO_2$ and acid-soluble metabolite (ASM) production was determined from the reaction buffer and normalized to liver sample wet weight. Liver acyl-carnitines concentrations were determined by LC-MS/MS, and ratios (B) of C2/C4 and C4/C16 were compared to assess complete FAO and □-oxidation, respectively. Values are means ± SEM (n=8). § $p<0.05$ interaction, * $p<0.05$ main effect HCR vs. LCR, † $p<0.05$ main effect LFD vs. WD, ** $p<0.05$ HCR vs. LCR within diet.

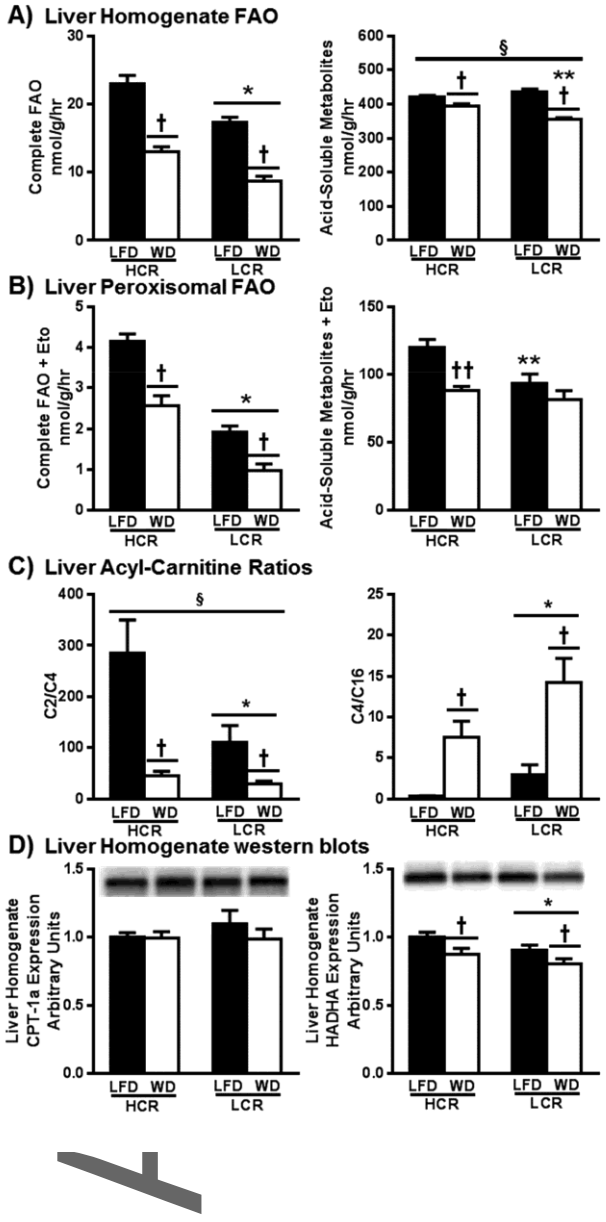

Figure 4 – Liver mitochondrial content, respiratory capacity, and hepatic NAD+/NADH ratio is higher in rats with high intrinsic aerobic capacity. In Figure 4A, markers of hepatic mitochondrial content and TCA cycle flux are presented as citrate synthase activity in liver homogenate and 2-[14C]-pyruvate oxidation to CO_2. Liver mitochondrial respiration was determined by measurement of O_2 consumption using a Clark electrode system in the presence of (B) glutamate (+malate and succinate) in different respiratory states (basal, state 3, and uncoupled). Hepatic NAD+, NADH, ATP, ADP, and AMP was determined by LC-MS/MS. (C) The mitochondrial energy state is represented as the ratio of NAD+ to NADH, and adenine energy charge. Values are means ± SEM (n=7-8). § $p<0.05$ interaction, * $p<0.05$ main effect HCR vs. LCR, † $p<0.05$ main effect LFD vs. WD, †† $p<0.05$ LFD vs. WD within strain.

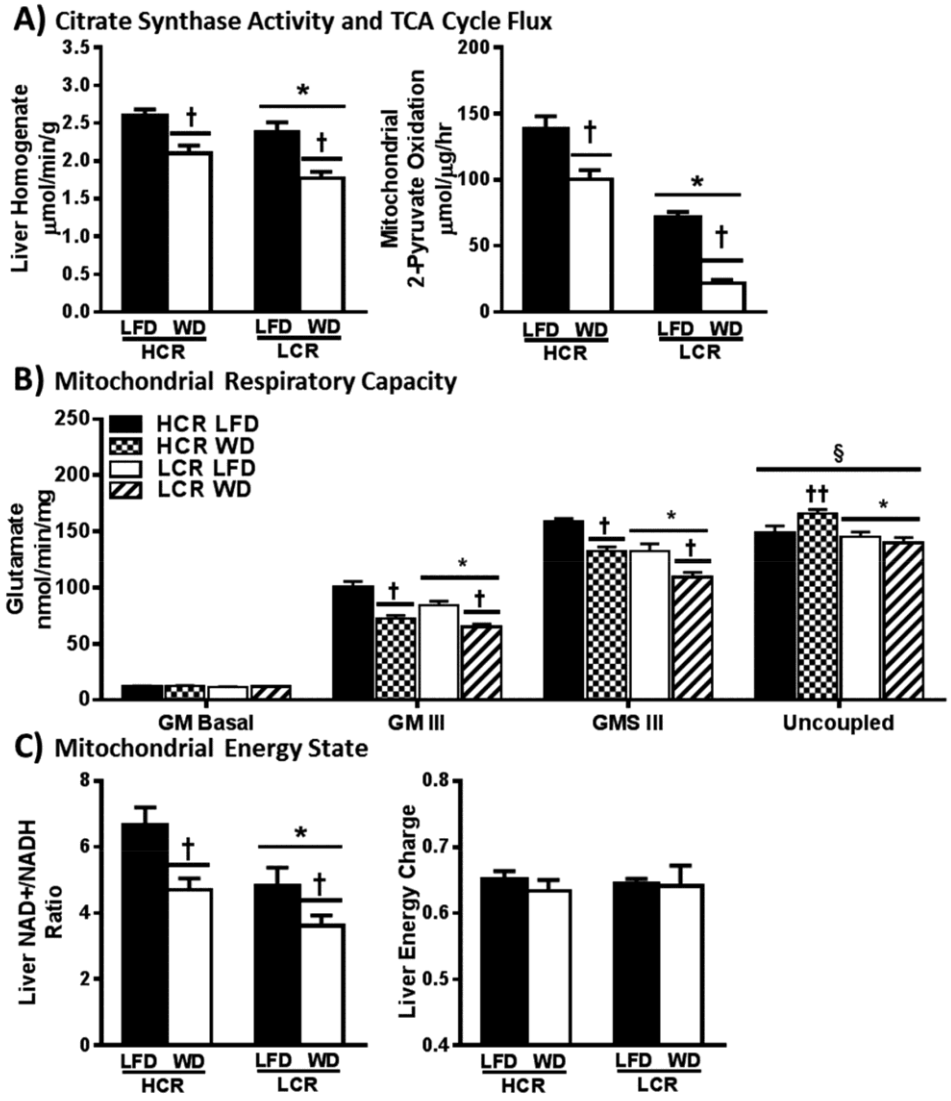

Figure 5 – Protein expression of markers of oxidative stress and anti-oxidant enzymes in isolated liver mitochondria are presented as means ± SEM (n=7-8): (A) 4-HNE, (B) SOD2, (C) UCP2, and (D) GPX1. § $p<0.05$ interaction, * $p<0.05$ main effect HCR vs. LCR, † $p<0.05$ main effect LFD vs. WD, ** $p<0.05$ HCR vs. LCR within diet, †† $p<0.05$ LFD vs. WD within strain.

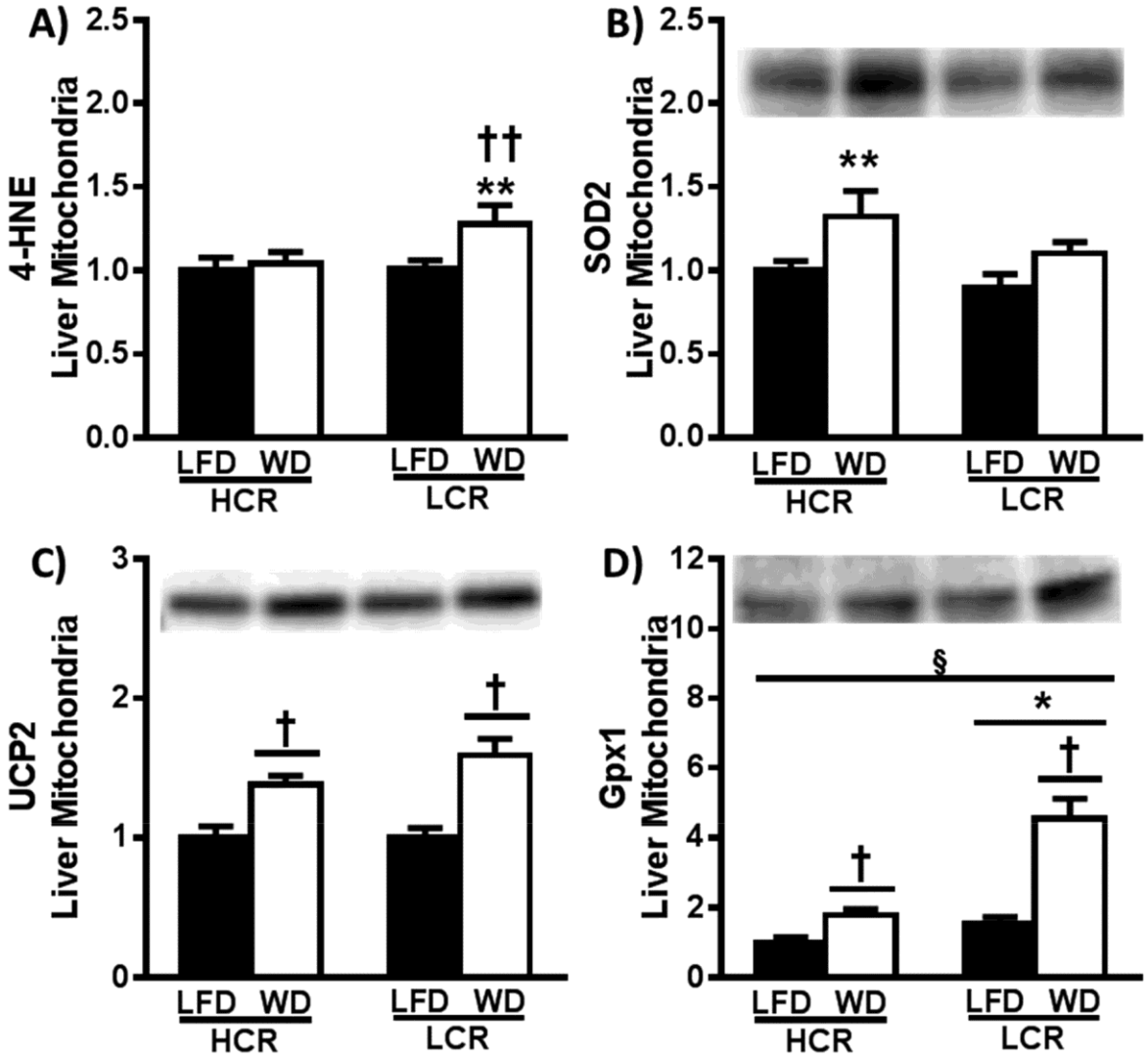

Figure 6 – Low intrinsic aerobic capacity increases susceptibility to liver mitochondrial localization of pro-apoptotic proteins and associated effector caspase activation. Mitochondrial localization of proteins involved in the regulation of mitochondrial outer mitochondrial membrane permeability were determined in isolated liver mitochondria by western blot analysis: (A) Anti-MOMP Opening (Bcl-2 & Bcl-xL), (B) Pro-MOMP Opening (Bax, Bak, and Cleaved BCL-xL). Liver expression of active (cleaved) effector caspases (C), caspase-3 and caspase-7), was determined in liver homogenate by western blot analysis. Representative blots (D). All values are presented as means ± SEM (n=7-8). * $p<0.05$ main effect HCR vs. LCR, † $p<0.05$ main effect LFD vs. WD, ** $p<0.05$ HCR vs. LCR within diet.